

**Representing Polyhedra:  
Faces are Better than Vertices**

*Lenwood S. Heath, Praveen K. Paripati,  
and John W. Roach*

**TR 92-20**

Department of Computer Science  
Virginia Polytechnic Institute and State University  
Blacksburg, Virginia 24061

April 29, 1992

# Representing Polyhedra: Faces are Better than Vertices

Lenwood S. Heath      Praveen K. Paripati

John W. Roach

Department of Computer Science

Virginia Polytechnic Institute & State University

Blacksburg, VA 24061

March 31, 1992

## Abstract

In this paper, we investigate the reconstruction of planar-faced polyhedra given their spherical dual representation. We prove that the spherical dual representation is unambiguous for all genus 0 polyhedra and that a genus 0 polyhedron can be uniquely reconstructed in polynomial time. We also prove that when the degree of the spherical dual representation is at most four, the representation is unambiguous for polyhedra of any genus. The first result extends, in the case of planar-faced polyhedra, the well known result that a vertex or face connectivity graph represents a polyhedron unambiguously when the graph is triconnected and planar. The second result shows that when each face of a polyhedron of arbitrary genus has at most four edges, the polyhedron can be reconstructed uniquely. This extends the previous result that a polyhedron can be uniquely reconstructed when each face of the polyhedron is triangular. As a consequence of this result, we prove that the 4-dimensional hypercube, a classic example of ambiguity in the wire frame representation scheme, is unambiguous when the same connectivity graph is viewed as the spherical dual representation of a polyhedron and thus that faces are a more powerful representation than vertices. A result of the reconstruction algorithm is that high level features of the polyhedron are naturally extracted. Both of our results explicitly use the fact that the faces of the polyhedron

are planar. We conjecture that the spherical dual representation is unambiguous for polyhedra of any genus.

**Keywords:** polyhedra, reconstruction, geometric dual, solid modeling, computer vision, CAD

## 1 Introduction

A common means of representing a 3-dimensional object is through the abstraction known as a polyhedron. A *polyhedral surface* is a closed surface (a 2-manifold) that partitions Euclidean 3-space  $E^3$  into 3 sets: (i) points inside the surface, (ii) points on the surface, and (iii) points outside the surface. A *polyhedron* is the set of points either inside or on a polyhedral surface. The *boundary* of the polyhedron is the polyhedral surface. Viewed combinatorially, the surface consists of a finite number of faces, edges, and vertices. Each edge is shared by exactly two faces, and each edge has exactly two vertices as its endpoints. Each face is a connected open set. The edges incident to any vertex appear on the surface in a cyclic order around the vertex. Alternately, the faces incident to the vertex appear in a cyclic order around the vertex, and two faces adjacent in the order share an edge incident to the vertex. We only consider polyhedra with planar faces; that is, each face is contained in a plane.

Constructive solid geometry views a polyhedron in terms of point sets, while boundary representations, as the name indicates, characterize a polyhedron based on its boundary [18]. Since the boundary consists of entities of various dimensions—faces, edges, and vertices—there are various schemes for representing a polyhedron. Obtaining a polyhedron from its representation is termed *reconstruction*. If there is always a single polyhedron that can be obtained from any representation in the representation scheme, the polyhedron is *uniquely reconstructible* in that representation scheme. The problem we consider in this paper is the unique reconstruction of polyhedra in a representation scheme that encodes the minimum amount of information required for reconstruction and that is useful for computer vision and other applications.

The spherical dual representation [19] is a representation scheme for polyhedra useful in both solid modeling and computer vision. The spherical dual representation of a polyhedron is a graph in which each face of the polyhedron is a node and is labeled by the equation of the plane containing the face. A node is connected by an arc to another if the two faces share an edge in the polyhedron. No ordering of the arcs around each node is specified. In fact, no explicit order information whatsoever is maintained. The spherical dual representation scheme can be viewed as the dual of the wire frame representation of polyhedra. Roach, Wright, and Ramesh [19] raise, but do not answer, the question of unique reconstructibility for this representation scheme.

In this paper, we investigate the reconstruction of a polyhedron from its spherical dual representation. It is well known that the wire frame representation (i.e., the vertex connectivity graph) of a polyhedron is ambiguous [15,18]. Also, given either the wire frame or face connectivity graph of a genus 0 polyhedron, algorithms are known to *uniquely* reconstruct it only when the graph is triconnected [6]. We extend these algorithms to uniquely reconstruct any genus 0 polyhedron, given its face connectivity graph (spherical dual representation). We prove that any spherical dual representation of degree at most 4 represents a polyhedron unambiguously. As a corollary to this result, we show that the face connectivity graph is not exactly the dual of the wire frame with regard to ambiguity. This is accomplished by an example (the four-dimensional hypercube) which is ambiguous as a wire frame, but which is unambiguous as a spherical dual representation. The results have an added importance since the spherical dual representation also has some interesting applications in computer vision. For example, the spherical dual representation provides some useful relationships between the representation of an object and its image under perspective projection [17].

The structure of the paper is as follows. The next section contains the necessary graph theoretic and topological definitions. Section 3 reviews previous work in solid modeling representation and reconstruction. In Section 4, we develop our algorithm for uniquely reconstructing a genus 0 polyhedron given its spherical dual representation. Section 5 proves that the spherical dual representation of any polyhedron having maximum degree 4 is unambiguous. In that section, we also prove, by an example, that the spherical dual

representation is a more powerful representation than the wire frame. The last section concludes with observations and conjectures.

## 2 Terms and Definitions

A *graph*  $G = (N, A)$  consists of a set of *nodes*  $N$  and a set of *arcs*  $A$ ; each arc is an unordered pair of distinct elements from  $N$ . (We have chosen this non-standard terminology for undirected graphs—nodes and arcs instead of vertices and edges—to avoid confusion between the vertices and edges of a polyhedron and the nodes and arcs of the associated spherical dual representation. Nodes and arcs are generally used in the context of directed graphs.) If  $A$  is a multiset, that is, if an arc may occur several times, then  $G$  is a *multigraph*. Multiple arcs between the same pair of nodes are called *parallel arcs*.

A *path*  $P$  between nodes  $v_0$  and  $v_k$  in a graph  $G$  is a sequence of nodes  $v_0, v_1, \dots, v_k$  such that  $(v_{i-1}, v_i) \in A$ ,  $1 \leq i \leq k$ . Path  $P$  is a *simple path* if  $v_0, v_1, \dots, v_k$  are distinct. A *cycle*  $C$  in  $G$  is a path  $v_0, v_1, \dots, v_k$  such that  $v_0 = v_k$ . Cycle  $C$  is a *simple cycle* if  $v_0, v_1, \dots, v_{k-1}$  are distinct. A graph  $G = (N, A)$  is *connected* if there exists a path between every pair of nodes in  $N$ . The number of arcs incident on a node  $v_i$  is called the *degree* of the node. Two arcs are said to be in *series* if they have exactly one node in common and if this node is of degree two. A node  $v \in N$  is an *articulation point* of a connected graph  $G = (N, A)$  if the subgraph induced by  $N - \{v\}$  is not connected. A connected graph  $G$  is *biconnected* if  $G$  contains no articulation point. A *biconnected component* of  $G$  is a maximal induced subgraph of  $G$  which is biconnected. Let  $v_1, v_2$  be a pair of nodes of a biconnected graph  $G = (N, A)$ ;  $\{v_1, v_2\}$  is a *separation pair* for  $G$  if the induced subgraph on  $N - \{v_1, v_2\}$  is not connected. A biconnected graph  $G$  is *triconnected* if  $G$  contains no separation pair. A *triconnected component* of  $G$  is a maximal induced subgraph of  $G$  which is triconnected. Hopcroft and Tarjan [8] give an algorithm to find the triconnected components of a graph in time linear in the size of the graph.

The *genus* of an orientable, compact surface is the maximum number of non-intersecting simple closed curves that can be removed from its surface without disconnecting it. Thus

the genus of a sphere is 0, and the genus of a torus is 1. In general, an orientable surface with  $g$  holes has genus  $g$ . The *genus* of a polyhedron is the genus of its surface.

A graph  $G$  is said to be topologically *embedded* in a surface  $S$  when it is drawn on  $S$  such that no two arcs intersect except at their common nodes (see Gross and Tucker [4]). If a graph is embedded in a surface, the complement of its image is a finite set of regions. A *face* of a topological embedding of  $G$  is a connected component of the complement of the image of  $G$ . (Henceforth, we use *facets*, rather than faces, to refer to the two-dimensional components of a polyhedron. We reserve *faces* to refer to the regions of a graph embedding.) The *genus* of a graph  $G$  is the genus of the orientable surface  $S$  of least genus such that  $G$  can be topologically embedded in  $S$ . A graph  $G$  is *planar* if  $G$  has an embedding in a plane (or, equivalently, in a sphere).

The *boundary* of a face  $f$  is the set of arcs in the (topological) closure of  $f$ . Two embeddings of a graph are *equivalent* when the boundary of a face in one embedding always corresponds to the boundary of a face in the other. The embedding of a graph on a surface is said to be *unique* if all its embeddings in that surface are equivalent. A planar graph has a unique planar embedding if and only if it is triconnected [25].

Given a connected graph  $G$ , a closed surface  $S$ , and an embedding  $i : G \rightarrow S$ , a *dual graph*  $G^*$  and a *dual embedding*  $i^* : G^* \rightarrow S$  are defined as follows. For each region  $f$  of the embedding  $i : G \rightarrow S$ , place a node  $f^*$  in its interior. Then, for each arc  $e$  of the graph  $G$ , draw an arc  $e^*$  between the nodes just placed in the interiors of the regions containing  $e$ . The resulting graph with nodes  $f^*$  and arcs  $e^*$  is called the *dual graph*  $G^*$  for the embedding  $i : G \rightarrow S$ . The resulting embedding of the graph  $G^*$  in the surface  $S$  is called the *dual embedding*. Whitney [25] shows that a triconnected planar graph has a unique planar embedding and hence a *unique* dual.

### 3 Representations

In this section, we review some representations that have been used in geometric modeling and in computer vision, including the spherical dual representation. We also review known

techniques for reconstructing a polyhedron from its representations.

### 3.1 Representations in Geometric Modeling

Geometric modeling is the art of creating data structures and algorithms capable of representing and calculating the three-dimensional physical shape of an object (Mantyla [15]). Requicha [18] identifies some important characteristics of a representation scheme for geometric modeling that have theoretical and practical implications:

1. *Domain*: The domain of a representation scheme characterizes the descriptive power of the scheme; the domain is the set of entities representable in the scheme.
2. *Validity*: The range of a representation scheme is the set of representations which are *valid*, that is, represent an actual "solid." A representation scheme is said to be *valid* if every representation in the scheme is valid.
3. *Completeness*: A representation is *unambiguous* or *uniquely reconstructible* if it corresponds to a single object. A representation scheme is *complete* if all of its valid representations are unambiguous.
4. *Uniqueness*: A representation of a solid is *unique* if it is the *only* representation for the solid in the scheme. A representation scheme is *unique* if all its valid representations are unique.

In this paper, we concentrate on the issue of whether a representation scheme is complete. As we are attempting to give a representation scheme using the least possible amount of information that yields an unambiguous representation for each object, completeness is the central characteristic considered here and the most difficult to prove.

The following are some of the common solid modeling schemes [15,18,21].

### 3.1.1 Wire Frame Representation

A wire frame model represents a solid object by representing its vertices and edges only. Each edge is typically represented by a six-tuple

$$\langle x_1, y_1, z_1, x_2, y_2, z_2 \rangle$$

giving the coordinates of the two endpoints  $(x_1, y_1, z_1)$  and  $(x_2, y_2, z_2)$  of the edge.

The main drawback of this representation scheme is its ambiguity. A wire frame model in general does not have enough information to represent an object uniquely (see Section 5). Characterizing it another way, two or more different objects can have the same set of edges. Thus wire frame representation is not a complete representation scheme.

### 3.1.2 Constructive Solid Geometry

The most general form of the constructive solid geometry (CSG) approach is the *half-space* model. In this model, solids are represented by a finite number of simple point sets called half-spaces that are combined by the standard set operations of *union*, *intersection* and *difference*.

The CSG representation scheme is complete but not unique.

### 3.1.3 Boundary Representations

Boundary representations represent a solid object by storing a description of its boundary. The boundary of an object divides space into two parts, one having finite volume and the other having infinite volume. If we assume that all objects have finite volume, then an object can be represented unambiguously by its boundary. The boundary is divided into a three-level hierarchy of entities: *facets*, *edges*, and *vertices*.

A widely used boundary representation is the solid modeling scheme based on Euler operators. Euler's formula for a convex polyhedron gives a relationship among the number of facets  $f$ , the number of edges  $e$ , and the number of vertices  $v$  of a convex polyhedron:



$v - e + f = 2$ . Define a *loop* of a facet to be a simple cycle of vertices and edges in the polyhedron that forms a connected component (in the topological sense) of the boundary of the facet. The boundary of every facet is composed of one external loop and zero or more internal loops. Euler's formula is generalized to an arbitrary polyhedron by introducing three additional parameters

1. The total number  $r$  of internal loops in the facets of the solid,
2. The genus  $g$  of the solid, and
3. The number  $s$  of disconnected components in a solid with a disconnected surface.

The general Euler's formula is  $v - e + f = 2 * (s - g) + r$ .

The operations used to construct the representation are called Euler operators because every operator used satisfies Euler's formula (e.g., two Euler operators are *mev*, for *make edge, vertex*, and *kef*, for *kill edge, face*). Mantyla [14] proves that Euler operators are sound and complete; that is, Euler operators create only meaningful models and every meaningful model can be constructed by Euler operators. Similar to the CSG scheme, boundary representations based on Euler operators are complete but not unique.

Representation schemes which are *both* unambiguous and unique are highly desirable because they are one-to-one mappings from the object space to the representation space. This implies that distinct representations in such schemes correspond to distinct objects, and therefore object equality may be determined by algorithms which compare object representations "syntactically" [18]. Both the CSG scheme and the boundary representation scheme are nonunique.

### 3.2 Representations in Computer Vision

Object representations in computer vision are generally surface based. We review some of the representation schemes used in computer vision and introduce the spherical dual representation.

A *Gaussian map* is a function that maps the surface onto a unit sphere. Each point  $x$  on a surface is mapped to a point  $y$  on the unit sphere such that the surface normal at  $x$  equals the surface normal at  $y$ . The unit sphere in this context is called the *Gaussian sphere*. The image of a surface  $S$  under the Gaussian map is called the *Gaussian image* of  $S$  [9]. In case of a convex surface with positive curvature everywhere, no two points on the surface have the same normal and the surface is recoverable from its Gaussian image up to scaling. In case of a general polyhedron, all points on a facet map to the same point on the Gaussian sphere. The Gaussian image represents the orientation of the object only. Size and shape information is lost, making it impossible to reconstruct the object from the Gaussian image. A popular extension of the Gaussian image representation is the *extended Gaussian image*. In this representation, each normal vector is weighted by the surface area of the corresponding facet.

Other important surface representations exploit a duality between points and planes in three dimensions. Duality is an important concept in geometry [1,7]. Dual space was originally proposed by Huffman as an aid in analyzing pictures of impossible objects [10] and later applied to interpreting general line drawings of polyhedral scenes [13,11]. Huffman's version of duality involves associating the plane

$$ax + by + cz + d = 0 \tag{1}$$

with the point  $(-a, -b, -d)$  in dual space. In addition to the duality between points and planes, there is also an induced duality between lines in  $(x, y, z)$ -space and lines in dual space. The dual of the line formed by the intersection of two planes is the line passing through the two points that are the duals of the planes. In Huffman's duality, only the first two coordinates of the dual point of a plane are related to orientation. *Gradient space*, another duality representation, is formed by orthogonally projecting the dual points  $(a, b, d)$  onto the plane  $d = 1$ . Shafer [22] provides extensive analysis describing the advantages and uses of duality and gradient space in analyzing images for computer vision. Unfortunately, the interesting relationships between lines and points in the image and the dual lines and points are achieved under the assumption that the images are produced by orthogonal projection.

The *spherical dual representation (SDR)* dualizes planes into points by normalizing the constant  $d$  to  $-1$  in Equation 1. This form of the dual transform is well known to mathematicians. Grunbaum [5] uses this transform to define a dual polyhedron when the given polyhedron is convex. Thus the plane

$$ax + by + cz - d = 0 \quad d \neq 0$$

is mapped to the dual point  $(a/d, b/d, c/d)$  in spherical dual space [19]. We name this dual the spherical dual since this normalization has spherical symmetry about the origin as opposed to the cylindrical symmetry of Huffman's duality. To represent a polyhedron, each facet is taken to be the point dual to the plane containing the facet. The dual point is the node of a graph called the *SDR* of the polyhedron. The node  $f$  corresponding to facet  $F$  is connected via an arc to the node  $f'$  corresponding to facet  $F'$  if facets  $F$  and  $F'$  share an edge. It is possible for two facets to share more than a single edge. The spherical dual representation does not explicitly represent such multiple adjacency and hence is not a multigraph. To accommodate multiple facets in the same plane, the spherical dual representation represents each facet as a different node in the graph; that is, two nodes carry the same label (planar equation) if the corresponding facets lie in the same plane. Henceforth, we identify each node in the *SDR* with its associated facet so that we can speak of a facet as *being* a node of the *SDR*. Figure 1 shows an object and its *SDR* (minus the planar equations). In view of the *graph* nature of the *SDR*, graph theoretic terms and operations apply to *SDR*. In fact, the spherical dual representation is the facet connectivity graph of the polyhedron, where each node has an attached planar equation. In contrast to the wire frame, the *SDR* is always a connected graph as long as the surface of the polyhedron is connected.

*Features* of an object are high level abstractions that humans generally identify and operate with. Some examples of object features in manufacture, design, and recognition are boss, rib, blind hole, and through hole. Feature extraction at this abstract level is thus important in object recognition and geometric modeling systems. These features are further abstracted into *projecting features* and *depressions*. Falcidieno and Giannini [3] present a method for the automatic recognition and representation of shape-based features in a

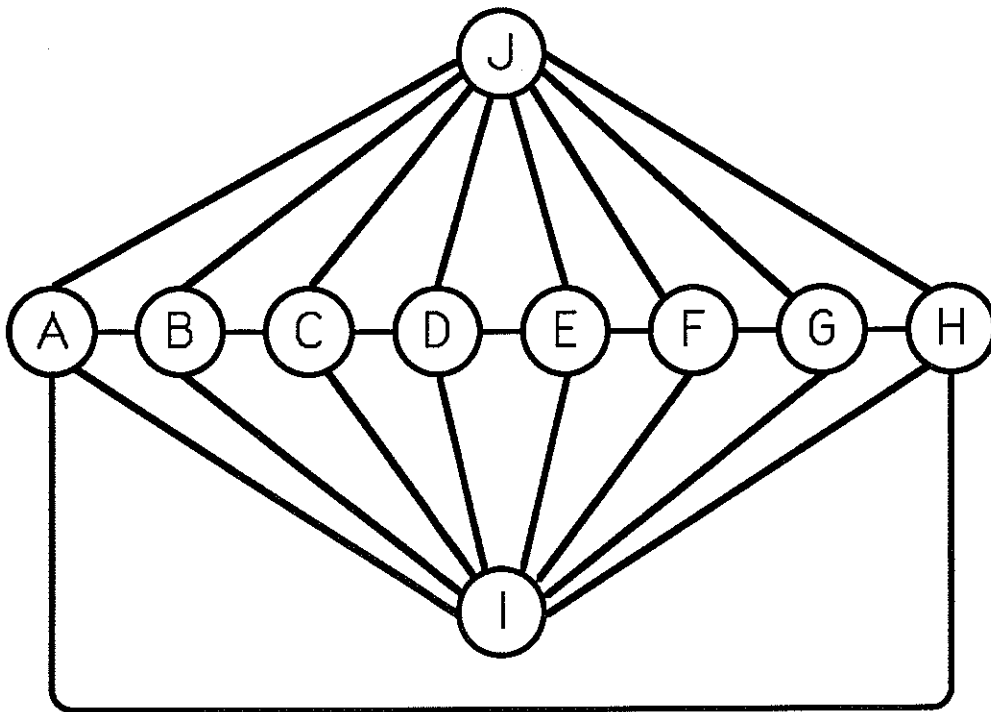
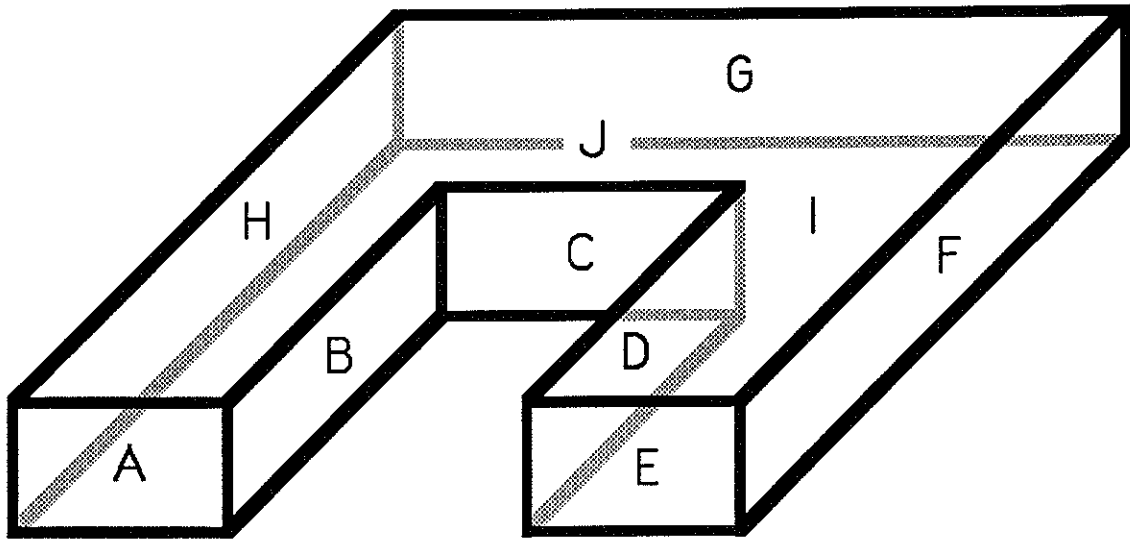


Figure 1: An object and its *SDR*

geometric modeling system. Loops in a face are the primary elements of this approach. The algorithm however requires the specification of the object as a face adjacency hypergraph, i.e., in addition to representing each face by a node and edges between faces by an arc between corresponding nodes, a hyperarc is defined for each vertex. Also each loop on a given face is organized into an ordered sequence of arcs. This also requires that their representation be a multigraph. The algorithm we present also extracts the shape features in terms of projecting features and depressions. Our method has the advantage that the specification of the object is only as a face adjacency graph rather than a face adjacency hypergraph. The loop information is extracted automatically. However, the domain of our algorithm is currently restricted to genus 0 objects only. The ability to extract high level features automatically makes our representation very powerful in computer aided manufacture and computer vision applications.

### 3.3 Reconstruction Techniques

Hanrahan [6] gives a linear time algorithm for the unique reconstruction of a genus 0 polyhedron given its wire frame representation. This algorithm, however, requires the wire frame input of the polyhedron to be triconnected and planar in the graph theoretic sense. The facets of the polyhedron correspond to the faces in the unique planar embedding of the wire frame.

Markowsky and Wesley [16] present an algorithm that generates all polyhedra with a given wire frame. This explicitly uses topological and geometric information by forcing the final facets to be planar. Human intervention is required to choose one of the several polyhedra reconstructed from such a wire frame representation.

Weiler [24] enumerates those boundary representations of polyhedra that are sufficient for unique reconstruction. Making use of Edmonds' Theorem [2], Weiler shows that knowing the *ordered* set of edges around each vertex, or each edge, or each facet of a polyhedron is sufficient information for the reconstruction of any polyhedron. Weiler also states that a representation without order has insufficient information for unique reconstruction. Later,

we show unique reconstructibility for genus 0 polyhedra when represented by *SDR*, a representation without order information. We also prove that a polyhedron of any genus that only has facets with at most 4 edges is uniquely reconstructible from its *SDR*.

A different approach to reconstruction of convex polyhedra is suggested by Minkowski's Theorem [5]. Minkowski uniquely characterizes, up to a translation, any convex polyhedron by the *area* of its facets and their orientations. Using the Minkowski and Brunn-Minkowski Theorems [5], Little [12] solves the problem of reconstructing the polyhedron, given its extended Gaussian image, by solving a constrained minimization problem. The domain of Little's algorithm is the same as that of Minkowski's Theorem; it fails to reconstruct non-convex polyhedra.

The most important result on the realization of a polyhedron from its wire frame is Steinitz's Theorem [5]. The theorem states that *a graph  $G$  is realizable as a convex polyhedron if and only if  $G$  is planar and triconnected*. In the case of reconstruction of polyhedra, this theorem can be used for all combinatorially convex polyhedra. A polyhedron is *combinatorially convex* if its wire frame is planar and triconnected and the polyhedron has genus 0. From Whitney's Theorem [25], every combinatorially convex polyhedron is uniquely reconstructible from its facet connectivity graph, i.e., its *SDR*. In the next section, we extend unique reconstructibility to *every* genus 0 polyhedron.

## 4 Reconstruction of Genus 0 Polyhedra

In this section, we present an algorithm RECONSTRUCT that uniquely reconstructs any genus 0 polyhedron  $P$  from its spherical dual representation. RECONSTRUCT first builds a graph for each facet in  $P$  and then extracts the vertices of each boundary of the facet from that graph.

Let  $SDR = (N, A)$  be the spherical dual representation of the genus 0 polyhedron  $P$ . Let  $\mathcal{P}(f)$  be the plane containing the facet  $f \in N$ . Each facet  $f$  of  $P$  consists of a bounded, connected region in  $\mathcal{P}(f)$  that has one or more cycles of edges and vertices of  $P$  as boundary. If  $f$  is bounded by  $t$  cycles, then  $f$  has exactly  $t - 1$  holes. To reconstruct  $P$ , it suffices

to determine all the bounding cycles of all facets. Let  $\mathcal{F}(f)$  be the set of facets that are adjacent to  $f$  in  $SDR$ . If  $f^* \in \mathcal{F}(f)$ , then  $\mathcal{L}(f, f^*) = \mathcal{P}(f) \cap \mathcal{P}(f^*)$  is an infinite line within  $\mathcal{P}(f)$  that contains the (one or more) edges of  $P$  that are shared by  $f$  and  $f^*$ .

Suppose that  $f^*, f^{**} \in \mathcal{F}(f)$  have the property that lines  $\mathcal{L}(f, f^*)$  and  $\mathcal{L}(f, f^{**})$  are not parallel. Then  $\mathcal{L}(f, f^*)$  and  $\mathcal{L}(f, f^{**})$  intersect at a point  $T(f, f^*, f^{**})$  within  $\mathcal{P}(f)$ . Let  $\mathcal{Q}(f)$  be the set of all such intersections within  $\mathcal{P}(f)$ . Then every vertex  $v$  of  $P$  that is incident to  $f$  is an element of  $\mathcal{Q}(f)$ . In general,  $\mathcal{Q}(f)$  contains many points that are not vertices of  $P$ . A necessary condition for a point  $p \in \mathcal{Q}(f)$  to be a vertex of  $P$  is that there exist a *defining cycle*  $f, f_1, \dots, f_k$  in  $SDR$  such that  $p \in \mathcal{Q}(f_i)$ ,  $i = 1, \dots, k$ . (Generalizing the  $T$  notation, we write  $p = T(f, f_1, \dots, f_k)$ .) If  $p$  is indeed a vertex of  $P$ , then there is, of course, a defining cycle for  $p$  which is the cycle of facets incident to  $p$ . However, a given point  $p$  may have many defining cycles. That the existence of a defining cycle is not sufficient for a point  $p$  to be a vertex is shown by the example in Figure 2. This example is a truncated tetrahedron, where the facet  $E$  has cut off the top vertex  $p$  of the original tetrahedron. The point  $p$  is not a vertex of the truncated tetrahedron, yet  $p \in \mathcal{Q}(A)$ ,  $p \in \mathcal{Q}(B)$ ,  $p \in \mathcal{Q}(C)$ , and  $A, B, C$  is a cycle in  $SDR$ .

If a point  $p \in \mathcal{Q}(f)$  meets the above necessary condition (of having a defining cycle), call  $p$  a *near-vertex*. The minimal subgraph  $\mathcal{NF}(f)$  of  $SDR$  that contains all defining cycles of every near-vertex of  $f$  is the *near-facet graph* of  $f$ . Clearly, every node in  $\mathcal{F}(f)$  is also adjacent to  $f$  in  $\mathcal{NF}(f)$ .

An outline of an algorithm for constructing  $\mathcal{NF}(f)$  for all  $f \in N$  follows. Let  $\mathcal{J}$  be the set of all lines in 3-dimensional space defined by edges in  $P$ :

$$\mathcal{J} = \{ \mathcal{L}(f_1, f_2) \mid (f_1, f_2) \in A \}.$$

Let  $\mathcal{I}$  be the set of all pairwise intersections of two distinct lines in  $\mathcal{J}$  such that each intersection is a single point:

$$\mathcal{I} = \left\{ T(f_1, f_2, f_3, f_4) \mid \begin{array}{l} \mathcal{L}(f_1, f_2), \mathcal{L}(f_3, f_4) \in \mathcal{J} \text{ and} \\ \left| \mathcal{L}(f_1, f_2) \cap \mathcal{L}(f_3, f_4) \right| = 1 \end{array} \right\}.$$

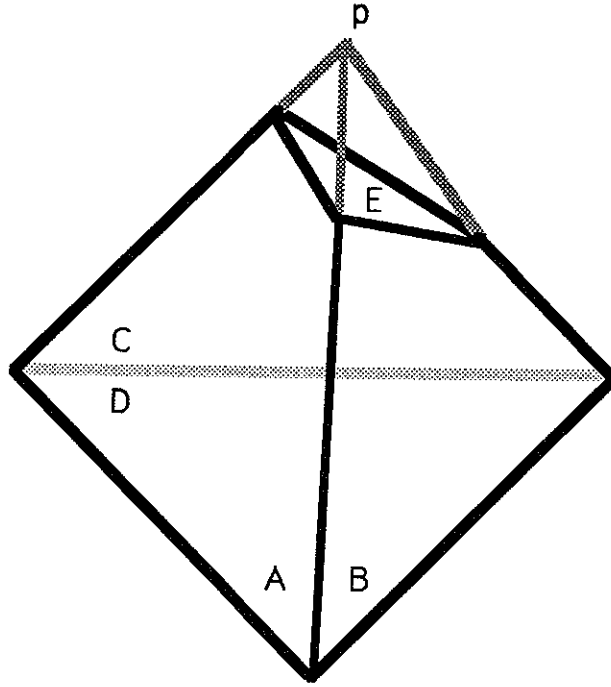


Figure 2: Truncated tetrahedron

Clearly, for each  $f \in N$ , we have  $\mathcal{Q}(f) \subset \mathcal{I}$ . The calculation of  $\mathcal{I}$  requires  $O(|A|^2) = O(|N|^2)$  time. For each  $p \in \mathcal{I}$ , build a subgraph  $\mathcal{H}(p)$  of  $SDR$  induced by this set of arcs:

$$\{(f_1, f_2) \mid p \in \mathcal{L}(f_1, f_2)\}.$$

In  $O(|N|)$  time per  $p \in \mathcal{I}$ , eliminate from  $\mathcal{H}(p)$  any arcs that do not appear in a cycle of  $\mathcal{H}(p)$  and any isolated nodes; the resulting graph is  $\mathcal{H}'(p)$ . Calculate the biconnected components of each  $\mathcal{H}'(p)$ . For a particular  $f \in N$ , consider every  $\mathcal{H}'(p)$  that contains  $f$ ; every biconnected component of  $\mathcal{H}'(p)$  that contains  $f$  is a subgraph of  $\mathcal{NF}(f)$ . In fact, all of  $\mathcal{NF}(f)$  is obtained by taking the union of all such biconnected components from every  $\mathcal{H}'(p)$  that contains  $f$ . The calculation of  $\mathcal{NF}(f)$  for all  $f \in N$  is accomplished in  $O(|N|^3)$  time. We emphasize that this is a worst case time complexity; under reasonable assumptions on the sizes of each  $\mathcal{NF}(f)$  and each  $\mathcal{H}(p)$ , the time complexity can be reduced to  $O(|N|^2)$ .



Shortly, we will be embedding subgraphs of  $\mathcal{NF}(f)$  in the plane and reading off the vertices incident to  $f$  from the faces of the embeddings. Any node of degree two in  $\mathcal{NF}(f)$  has no effect on these embeddings and can be eliminated by *series reduction* (replace the node and its two incident arcs by a single arc; see Gross and Tucker [4]). If any parallel arcs are introduced by series reduction, all but one can be eliminated by *parallel reduction*.

There is one last kind of reduction that can be applied to  $\mathcal{NF}(f)$  without losing the ability to recover the vertices on the boundary of  $f$ . Suppose  $\{f_1, f_2\} \subset N - \{f\}$  is a separation pair of  $\mathcal{NF}(f)$ . Let  $C$  be any component of  $\mathcal{NF}(f) - \{f_1, f_2\}$  that does not contain  $f$ . Let  $f^*$  be a node in  $C$ . Since every defining cycle containing  $f^*$  must pass through  $f$ ,  $f_1$ , and  $f_2$ , the plane  $f^*$  passes through  $T(f, f_1, f_2)$ . Therefore, every node of  $C$  passes through  $T(f, f_1, f_2)$ ; in a geometric sense, the nodes of  $C$  give only redundant information. In a graph theoretic sense, observe that any face in a planar embedding of  $\mathcal{NF}(f)$  that is incident on a node of  $C$  is also incident on  $f_1$  and  $f_2$ . A *separation-pair reduction* deletes  $C$  and adds an arc between  $f_1$  and  $f_2$ . By the above discussion, such a reduction does not affect the information available for recovering vertices on the boundary of  $f$ .

The *facet graph*  $SDR(f)$  of  $f$  is  $\mathcal{NF}(f)$  that has been reduced as much as possible by series, parallel, and separation-pair reductions. As  $SDR$  is planar,  $\mathcal{NF}(f)$  is a subgraph of  $SDR$ , and  $SDR(f)$  is a reduction of  $\mathcal{NF}(f)$ ,  $SDR(f)$  is also planar. Also, every node in  $\mathcal{F}(f)$  is a node of  $SDR(f)$ . As calculating triconnected components can be accomplished in linear time [8], the reduction of  $\mathcal{NF}(f)$  to  $SDR(f)$  can be accomplished in  $O(|N|)$  time.

Since  $P$  has genus 0,  $SDR(f)$  gives us all the information necessary to determine the bounding cycles of  $f$ . For example, the number of bounding cycles is just the number of biconnected components of  $SDR(f)$ . This is illustrated in Figure 3 where facet  $F$  has two bounding cycles, and  $SDR(F)$  has two biconnected components. Observe also that  $F$  is the sole articulation point of  $SDR(F)$ . This observation is formalized in the following theorem.

**Theorem 1** *Let  $SDR = (N, A)$  be the spherical dual representation of a genus 0 polyhedron  $P$ , and let  $f$  be a node of  $SDR$ . If  $SDR(f)$  contains an articulation point, then  $f$  is the*

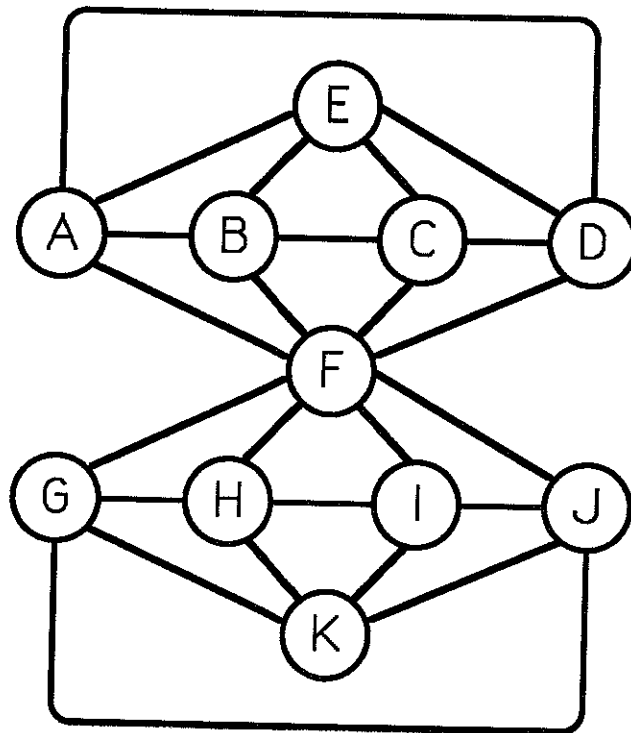
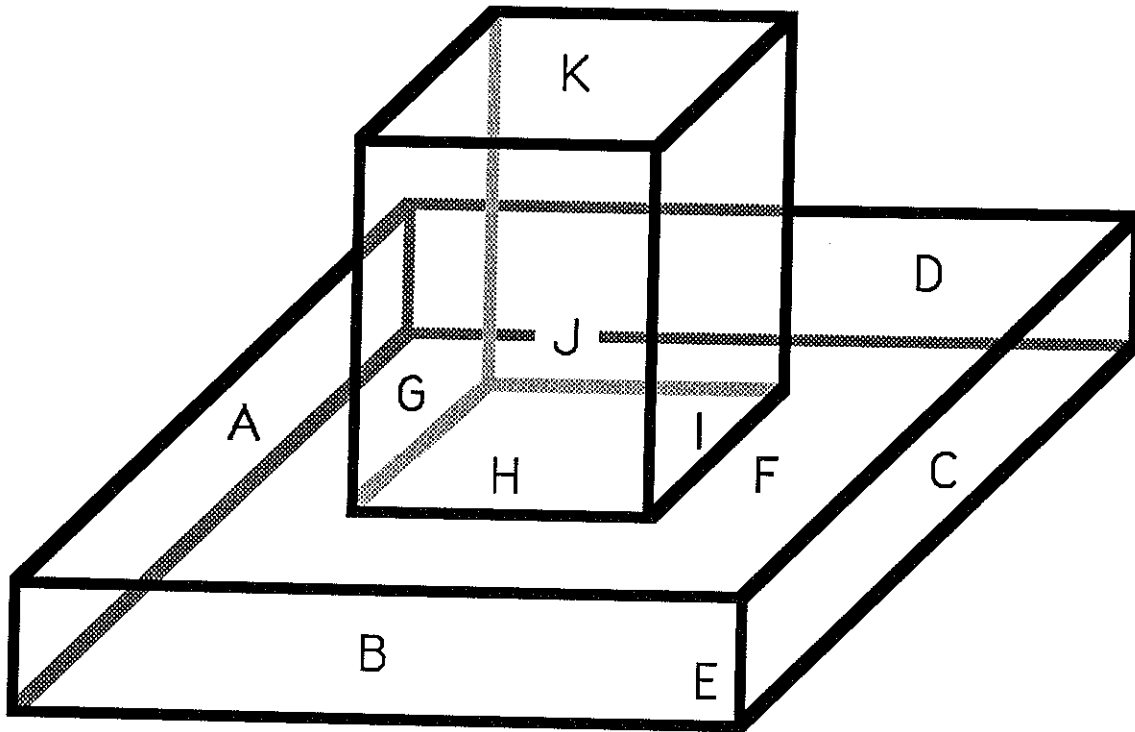


Figure 3: A polyhedron with an articulation point in its *SDR*

only articulation point.  $SDR(f) - f$  has  $t$  connected components if and only if  $f$  has  $t$  bounding cycles.

*Proof:* By the definition of  $SDR(f)$ , every node  $f^*$  in  $\mathcal{NF}(f) - \{f\}$  has two vertex disjoint paths to  $f$  in  $SDR(f)$ . Therefore, only  $f$  can be an articulation point of  $SDR(f)$ .

Assume that  $f$  has  $t$  bounding cycles. Define an equivalence relation  $\equiv$  on  $N - \{f\}$  such that  $f^* \equiv f^{**}$  if there exists a curve on (the surface of)  $P$  that goes from a point in the interior of  $f^*$  to a point in the interior of  $f^{**}$  without passing through the closure of  $f$  (that is, the curve avoids  $f$  and its boundary). Because  $P$  has genus 0,  $\equiv$  has exactly  $t$  equivalence classes.  $\mathcal{NF}(f) - f$  has one component for each equivalence class. It is easy to see that series, parallel, and separator-pair reductions apply independently to each component of  $\mathcal{NF}(f) - f$ . Thus,  $SDR(f) - f$  has the same number of components as  $\mathcal{NF}(f) - f$ , namely  $t$ . □

As  $SDR$  is planar but not necessarily triconnected,  $SDR$  does not have, in general, a unique embedding in the plane, whose dual would be the wire frame of  $P$ . A first approach that is doomed to failure is to decompose  $SDR$  into its triconnected components, embed each in the plane, and somehow read off the structure of  $P$  from these embeddings. The failure of this approach is illustrated by the polyhedron in Figure 4, shown with its  $SDR$ . The triconnected components of  $SDR$  are shown embedded in the plane in Figure 5. There is no face in any of the embeddings that corresponds to the vertex of  $P$  shared by the facets  $F, C, I,$  and  $H$ , nor to the vertex shared by the facets  $F, C, I,$  and  $J$ . However, there is a “false” vertex indicated by the face bounded by the cycle of facets  $F, H, I, J$ .

In view of this failure, we turn to facet graphs for a solution. From the proof of Theorem 1, we know that if  $SDR(f)$  has biconnected components  $C_1, C_2, \dots, C_t$ , then each  $C_i$  contains  $f$  and corresponds precisely to one of the bounding cycles of  $f$ . As each  $C_i$  may be processed separately to determine its corresponding bounding cycle, we henceforth assume that  $SDR(f)$  contains only one biconnected component, namely  $SDR(f)$  itself.  $SDR(f)$  can be decomposed into its biconnected components in linear time using depth-

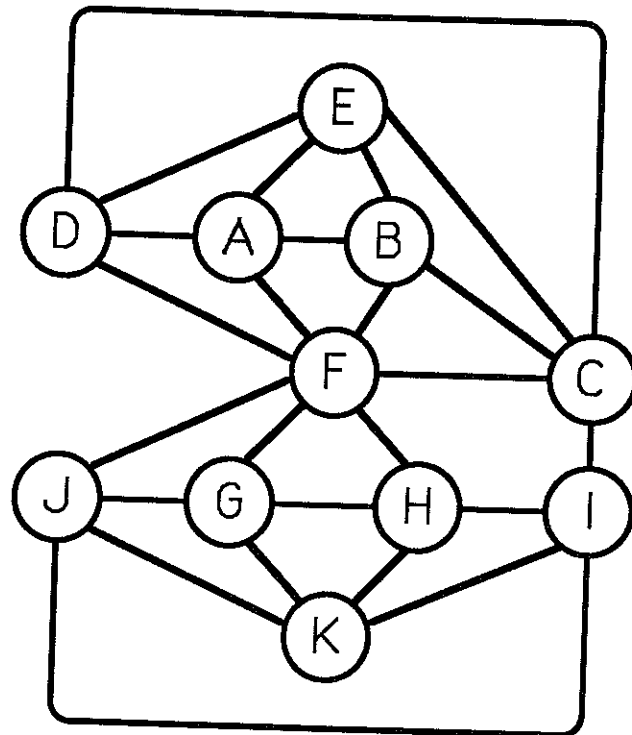
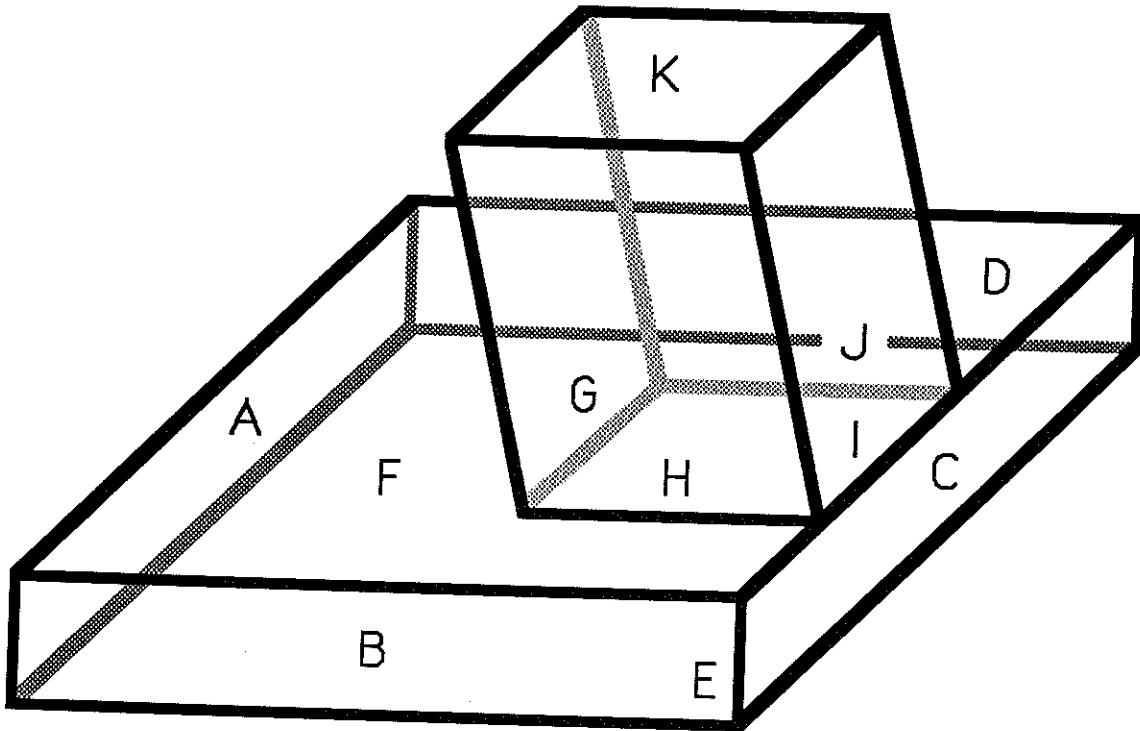


Figure 4: A polyhedron whose *SDR* is not triconnected

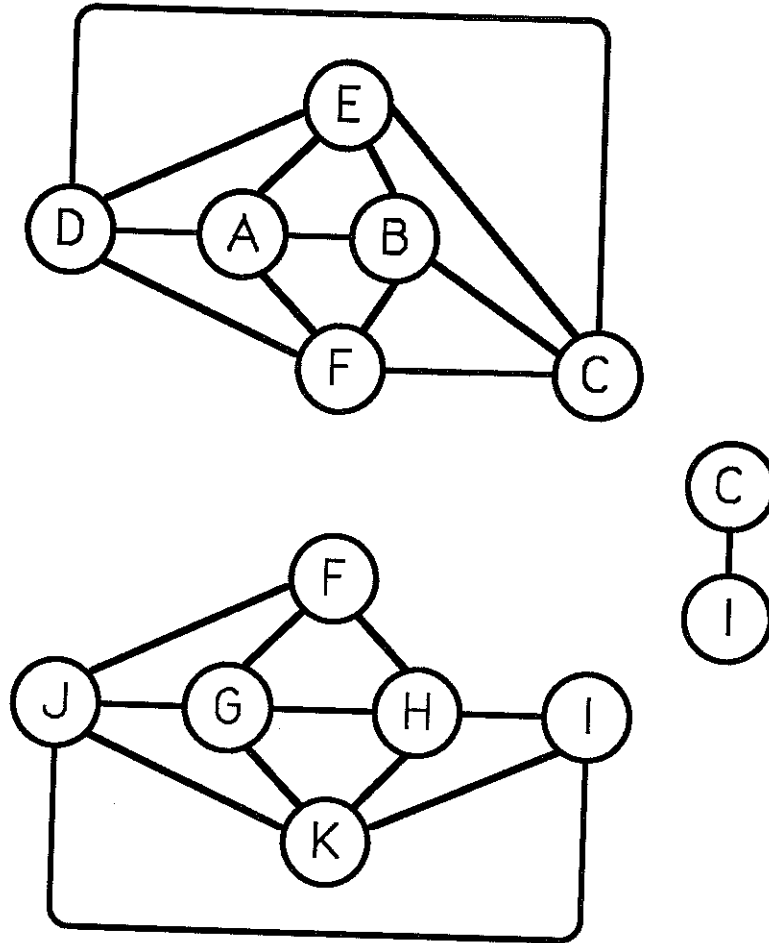


Figure 5: The corresponding triconnected components

first search (Tarjan [23]).

The bounding cycle of  $f$  is given by the sequence of vertices defining it, say,

$$v_1, v_2, \dots, v_k.$$

Each  $v_i$  has a defining cycle given by the actual facets that are incident to  $v_i$ :

$$f, f_{i,1}, f_{i,2}, \dots, f_{i,r(i)},$$

where  $f_{i,r(i)} = f_{i+1,1} \in \mathcal{F}(f)$ , for  $1 \leq i \leq k-1$ , and  $f_{k,r(k)} = f_{1,1} \in \mathcal{F}(f)$ . From these cycles we derive another cycle in  $\mathcal{NF}(f)$  that avoids  $f$  but otherwise goes along the bounding

cycle of  $f$ :

$$f_{1,1}, f_{1,2}, \dots, f_{1,r(1)} = f_{2,1}, \dots, f_{2,r(2)} = f_{3,1}, \dots,$$

$$f_{i-1,r(i-1)} = f_{i,1}, f_{i,2}, \dots, f_{i,r(i)} = f_{i+1,1}, \dots, f_{k,r(k)} = f_{1,1}.$$

This cycle in  $\mathcal{NF}(f)$  is reduced to a cycle  $\mathcal{C}(f)$  in  $SDR(f)$ , called the *neighborhood cycle* of  $f$ . Note that  $\mathcal{C}(f)$  need not be a simple cycle.

It is now our task to determine the vertices that occur on the bounding cycle of  $f$  and the order in which they occur. If  $SDR(f)$  is triconnected, then it has a unique planar embedding. Suppose that the order of the nodes in  $\mathcal{F}(f)$  about  $f$  in this embedding is  $f_1, f_2, \dots, f_k$  (note that these are not necessarily distinct). These correspond to the vertices

$$v_1 = T(f, f_1, f_2), v_2 = T(f, f_2, f_3), \dots, v_k = T(f, f_k, f_1),$$

in that order, defining the bounding cycle of  $f$ . Call this cycle of vertices the *cycle induced by the embedding*.

If  $SDR(f)$  is not triconnected, then it may not be true that all embeddings induce the same cycle of vertices or even that there exists an embedding that induces a cycle equal to the bounding cycle of  $f$ . We observe that:

**Lemma 2** *If  $SDR(f)$  is biconnected, then any separation pair of  $SDR(f)$  contains  $f$ .*

*Proof:* Since there is no separation-pair reduction that can be applied to  $SDR(f)$ , the Lemma follows. □

Thus any separation pair of  $SDR(f)$  has the form  $(f, f^*)$ , where  $f^*$  is a node of  $SDR(f)$  which may or may not be adjacent to  $f$ . Call  $f^*$  a *separation partner* of  $f$ . All separation partners of  $f$  can be identified by finding the articulation points of  $SDR(f) - f$  in linear time using depth-first search. For example, Figure 6 shows the facet graph of the facet  $F$  in the polyhedron of Figure 4. The separation partners of  $f$  are facets  $C$  and  $I$ . Note that  $F$  and  $C$  are adjacent in  $SDR(f)$ , while  $F$  and  $I$  are not.

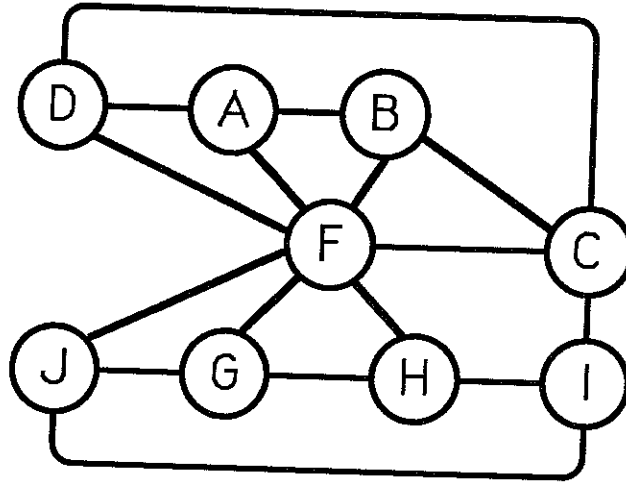


Figure 6: The facet graph  $SDR(F)$

The example in Figure 4 is a degenerate one in that  $\mathcal{P}(F)$ ,  $\mathcal{P}(C)$ , and  $\mathcal{P}(I)$  intersect in a single line. Figure 7 shows another example in which there is a single separation pair whose nodes are not adjacent. The polyhedron is a box with a raised pyramid (facets  $C$ ,  $D$ ,  $E$ , and  $F$ ) on its front face. Facets  $A$  and  $B$  are distinct facets that reside in the same plane and that are not adjacent in  $SDR$ . Facet  $B$  is a separation partner of  $A$  (and vice versa). Note that  $A$  and  $B$  share (are incident to) both vertices  $v_1$  and  $v_2$ . This is a general phenomenon:

**Lemma 3** *If  $f^*$  is a separation partner of  $f$  and  $f^* \notin \mathcal{F}(f)$ , then  $f$  and  $f^*$  have two or more shared vertices but no shared edges.*

*Proof:* Since  $f^* \notin \mathcal{F}(f)$ ,  $f$  and  $f^*$  do not share an edge.

Since  $f^*$  is in at least one cycle of  $SDR(f)$  that also contains  $f$ , and  $f^*$  is an articulation point of  $SDR(f) - f$ , there is some face containing both  $f$  and  $f^*$  in every planar embedding of  $SDR(f)$ . Therefore,  $f$  and  $f^*$  share at least one vertex. In particular,  $f^*$  occurs in the neighborhood cycle  $\mathcal{C}(f)$ . Since every node in  $\mathcal{F}(f)$  occurs in  $\mathcal{C}(f)$ , and  $f^*$  is an articulation point of  $SDR(f) - f$ ,  $f^*$  must occur at least twice in  $\mathcal{C}(f)$ . Otherwise, the removal of  $f^*$  from  $SDR(f) - f$  leaves  $\mathcal{C}(f)$ , and hence  $SDR(f) - f$ , connected.

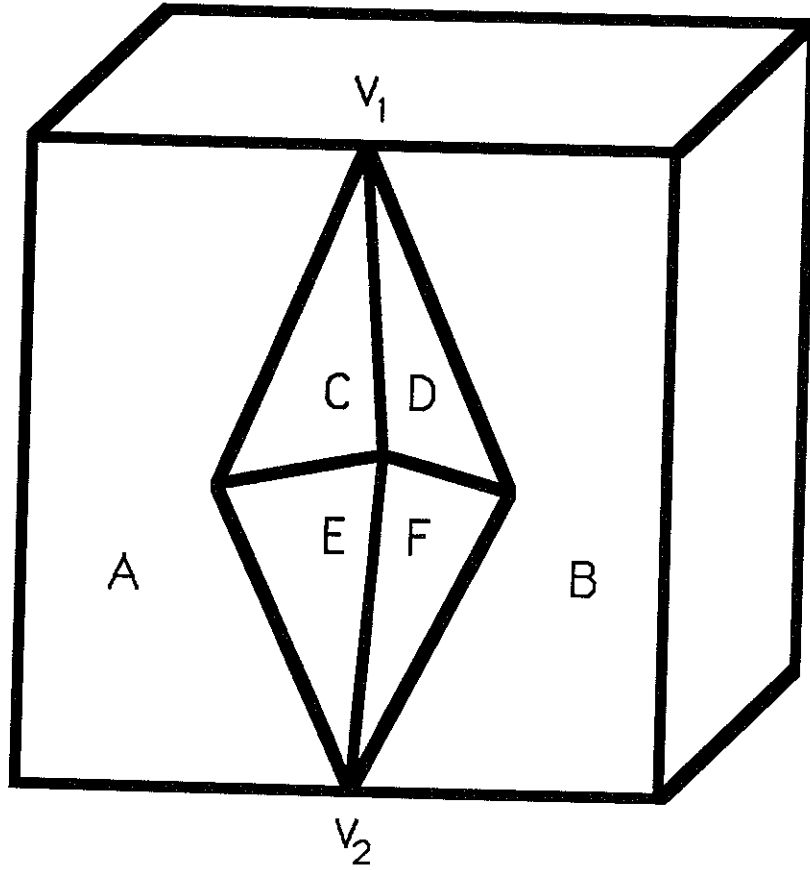


Figure 7: A separation pair whose nodes are not adjacent

Since  $f^*$  occurs at least twice in  $\mathcal{C}(f)$ ,  $f$  and  $f^*$  must share two or more vertices.  $\square$

We can make a stronger observation. Let  $f^*$  be a separation partner of  $f$ . Suppose  $SDR^*$  is a connected component of  $SDR(f) - f - f^*$ . Then there exists a closed curve contained in the closure (in the topological sense) of  $f \cup f^*$  that separates  $P$  into two regions, each homeomorphic to a disk, such that  $SDR^*$  is contained wholly in one of the regions and the remainder of  $SDR(f) - f - f^*$  is contained wholly in the other region.

$SDR^*$  may or may not contain a separation partner of  $f$ . If it does not, then we can determine the boundary between  $f$  and  $SDR^*$  as follows. Construct the *decomposition*



graph  $SDR^*(f^*)$  by taking the subgraph of  $SDR(f)$  induced on  $f, f^*$ , and the nodes of  $SDR^*$ , and add the arc  $(f, f^*)$  if  $f^* \notin \mathcal{F}(f)$ . The following observation is key.

**Lemma 4** *If  $SDR^*$  contains no separation partner of  $f$ , then  $SDR^*(f^*)$  is triconnected.*

*Proof:* Suppose  $SDR^*(f^*)$  is not triconnected and that  $(f_1, f_2)$  is a separation pair of  $SDR^*(f^*)$ . Then  $(f_1, f_2)$  is also a separation pair of  $SDR(f)$ . Since  $SDR(f)$  is separation-pair reduced, either  $f_1$  or  $f_2$  equals  $f$  and the other is a separation partner of  $f$ .  $\square$

Hence,  $SDR^*(f^*)$  has a unique planar embedding. The order of arcs in  $\mathcal{F}(f)$  around  $f$  in this embedding exactly gives the order in which facets of  $SDR^*(f^*)$  appear in the boundary between  $f$  and  $SDR^*$ . As is true when  $SDR(f)$  is triconnected, the cycle induced by the embedding gives the (cyclic) order of vertices and edges that form the bounding path. The cycle breaks into a path at the arc  $(f, f^*)$ .

For example, if we apply this decomposition to the facet graph  $SDR(F)$  in Figure 6, we obtain two decomposition graphs as shown in Figure 8. The arc  $(F, I)$  has been added to the lower decomposition graph. From the two planar embeddings, we learn the ordering of the vertices and edges in each of the two intermediate cycles  $C_1$  and  $C_2$  on  $F$ . One bounding cycle,  $C_1$ , of  $F$  has facets  $A, B, C$ , and  $D$  in that order and facets  $G, H, I$ , and  $J$  in that order in  $C_2$ . These two cycles are mated geometrically, obtaining a unique cycle  $C = (C_1 \cup C_2 - C_1 \cap C_2)$ , which is the bounding cycle of  $F$ . Viewed in terms of paths, they begin and end at the separation partners of  $F$ .

For any  $SDR(f)$  that is not triconnected, there always exists an  $SDR^*$  that contains no separation partner for  $f$  (examine the tree of biconnected components and articulation points of  $SDR(f) - f$  to find a biconnected component that is a leaf). We can then determine the subpath of the bounding cycle of  $f$  that is between  $f$  and  $SDR^*$  by the above decomposition method. Once the subpath is determined, we would like to remove  $SDR^*$  from further consideration. This can be done by replacing  $SDR(f)$  by the *reduced graph*  $SDR(f) - SDR^*$  with the arc  $(f, f^*)$  added, if  $f^* \notin \mathcal{F}(f)$ . In geometric terms, this

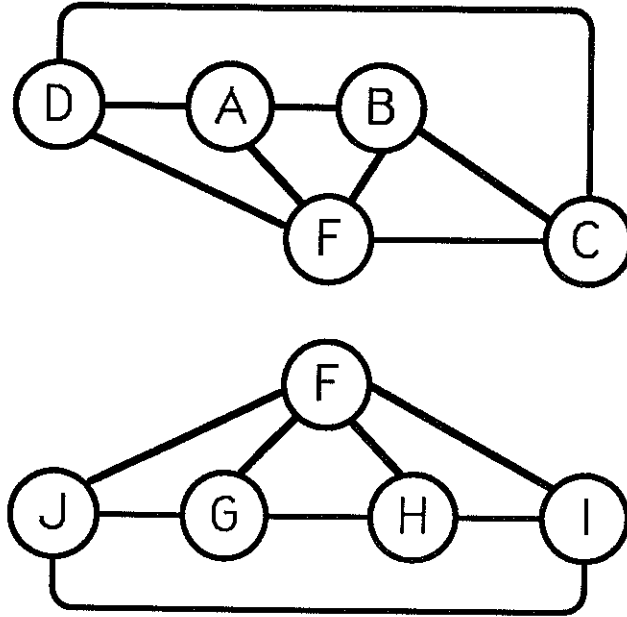


Figure 8: The decomposition graphs of  $SDR(F)$

reduction amounts to removing the feature of  $P$  that corresponds to  $SDR^*$  and replacing it by an edge in  $P$  shared by  $f$  and  $f^*$ . Geometrically this may not always work, as witnessed by the polyhedron in Figure 7, where facets  $A$  and  $B$  are in the same plane and therefore cannot share an edge. However, combinatorially the reduction does work. As stated earlier, the reduction reveals the structure of the polyhedron at a high level.

The strategy for finding the bounding cycle of  $SDR(f)$  now is clear. Iteratively find a decomposition graph  $SDR^*(f^*)$  that contains no separation partner of  $f$ , determine the corresponding bounding path, and reduce  $SDR(f)$ . Once  $SDR(f)$  is reduced to a triconnected graph, construct the bounding cycle of  $f$  by gluing the subpaths together at the separation partners of  $f$ . This completes the description of the processing of each biconnected component of  $SDR(f)$ .

In summary, the algorithm RECONSTRUCT consists of the following steps, applied to each facet  $f$ .

1. Form the set  $\mathcal{Q}(f)$ .

2. Determine  $\mathcal{NF}(f)$  and reduce it to  $SDR(f)$ .
3. Decompose  $SDR(f)$  into its biconnected components; say these components are  $SDR_1, SDR_2, \dots, SDR_k, k \geq 1$ .
4. For each biconnected component  $SDR_i$ , determine the bounding cycle of  $f$  corresponding to  $SDR_i$ , using the decomposition graph strategy.

The time complexity is dominated by the determination of  $\mathcal{NF}(f)$  for all  $f \in N$ ; this step has time complexity  $O(|N|^3)$ , as discussed earlier in this section. Determining  $\mathcal{NF}(f)$  and reducing it to  $SDR(f)$  only takes linear time. Finding the biconnected components is the same complexity as finding the articulation points of  $SDR(f) - f$ . Embedding a triconnected component is again a linear time operation. As the size of  $SDR(f)$  may be  $\Theta(|N|)$ , the time complexity of these steps for each facet is  $O(|N|)$ . The total time complexity for RECONSTRUCT is  $O(|N|^3)$ , though we expect that it is typically much less.

**Theorem 5** *Algorithm RECONSTRUCT uniquely reconstructs any genus 0 polyhedron given its SDR. The time complexity of RECONSTRUCT is  $O(|N|^3)$ .*

Algorithm RECONSTRUCT successfully reconstructs some, but not all, polyhedra of genus greater than zero. If  $P$  is a polyhedron of arbitrary genus, then it is possible that, for some facet  $f$ ,  $SDR(f)$  is not even planar. This occurs when (one or more) cycles in  $SDR(f)$  pass through (one or more) holes in  $P$ . Also, a facet  $f$  with multiple bounding cycles need not even be an articulation point in  $SDR(f)$  if a hole of  $P$  passes through  $f$ .

RECONSTRUCT can be modified to successfully reconstruct more polyhedra of genus greater than zero as follows. Typically, the facets in some non-empty subset of  $N$  can be successfully reconstructed by the steps in RECONSTRUCT. Boundary information from these reconstructed facets can be shared with neighboring facets that are not immediately reconstructible, perhaps making them reconstructible in the process. If such information sharing propagates to all facets of  $P$ , then the modified RECONSTRUCT successfully reconstructs  $P$ . We have found that this modified algorithm is capable of reconstructing a

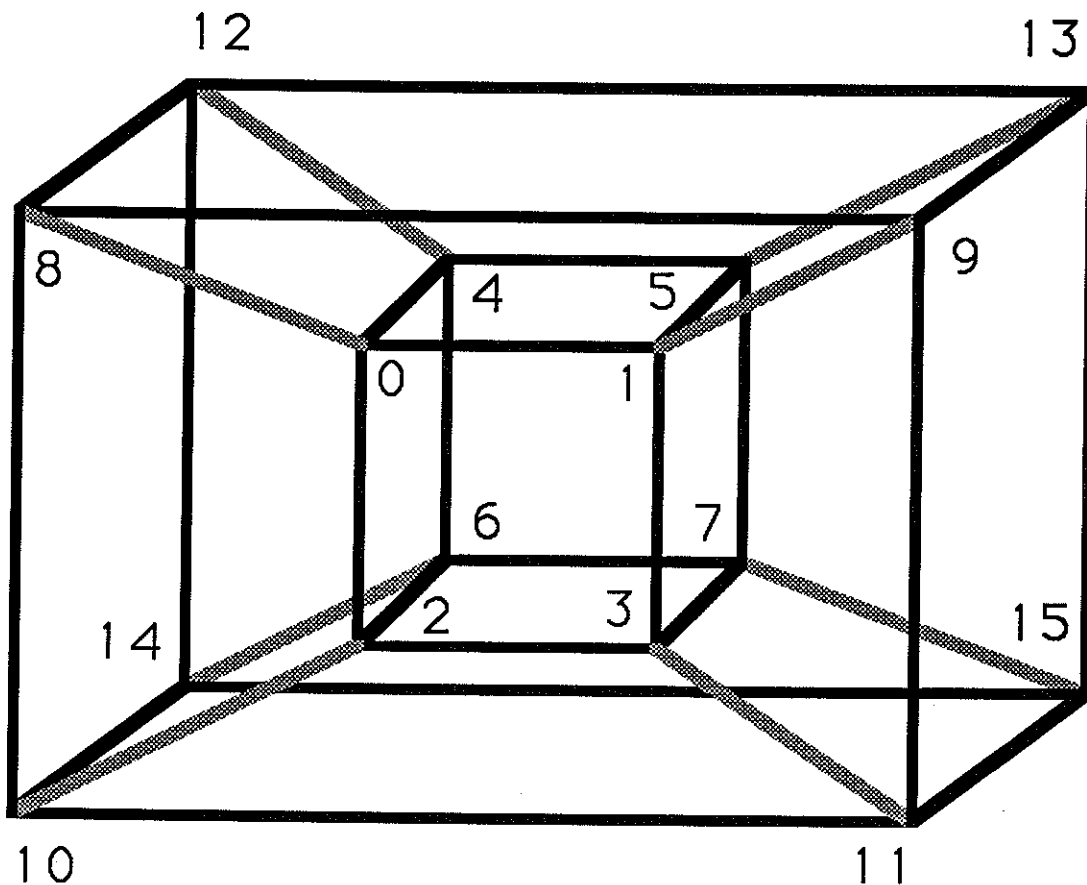


Figure 9: The degree four *SDR*

number of “hard” polyhedra that we had proposed as potential counterexamples to unique reconstructibility for polyhedra of higher genus.

The *SDR* shown in Figure 9 is a graph that cannot be solved by the above (modified) algorithm. The genus of this graph is 1. The *SDR*( $f$ ) of each facet of the polyhedron is non-planar and triconnected (each *SDR*( $f$ ) is homeomorphic to  $K_5$ ). Hence not even a single face can be reconstructed via planar embedding of its *SDR*( $f$ ). In the next section, however, we show that the graph in Figure 9 does have a unique reconstruction from its *SDR*.

## 5 SDRs of Maximum Degree 4

In this section, we show that an *SDR* of degree four represents a unique polyhedron. We also provide an algorithm to reconstruct the polyhedron from its *SDR*.

Each facet of a polyhedron having Figure 9 as *SDR* is connected by an arc to four other facets. Since each facet is connected to four other facets, each facet must be a quadrilateral. If the bounding cycle of each facet is determined, then the polyhedron represented by this *SDR* is reconstructed. We study the different quadrilaterals that can be formed by the adjacent facets. Consider the arrangement of four lines in a plane. In case of degeneracies among the four lines, there may not be any quadrilateral formed by these lines, for example when three of these lines are concurrent. On the other hand, if two of the lines are parallel, at most one quadrilateral is formed and the reconstruction of this facet is unambiguous.

The four lines defined by the facet adjacencies form two different quadrilaterals when the four lines are in general position. Refer to Figure 10 which depicts the plane containing facet 1 and the four lines formed by intersection with the planes containing facets 0, 3, 5, and 9. There are two possible interpretations for the boundary of each facet. One interpretation has vertices  $a$ ,  $f$ ,  $b$ , and  $e$ , while the other interpretation has vertices  $a$ ,  $d$ ,  $b$ , and  $c$ . Two vertices,  $a$  and  $b$ , are present in both interpretations. Vertex  $a$ , called the *fixed vertex*, has its context unchanged, i.e., when we follow the boundary of the two polygons in the same direction, the line segments occur in the same order. Vertex  $b$ , called the *reflex vertex*, has its context reversed. The internal angle at the reflex vertex changes from being a convex angle ( $\angle dbc$ ) in one interpretation to concave ( $\angle fbe$ ) in the other. It is immediately clear from Figure 10 that fixing any one of the remaining four vertices determines the polygon unambiguously. These four vertices are termed the *transient vertices*. Vertices on each of the lines through the fixed vertex and nearer the fixed vertex are called *intruded vertices* and those farther away are called *extruded vertices*. Thus in facet 1 in Figure 10, vertices  $c$  and  $d$  are intruded vertices and  $e$  and  $f$  are extruded vertices.

Given an arrangement of four lines in a plane, the following procedure can be used to classify a vertex as reflex, fixed, or transient. Four lines in general position determine six

(potential) vertices. The vertex that lies inside the convex hull defined by the six vertices is the reflex vertex. It is easy to see that there is exactly one such vertex. In Figure 10, the vertex formed by lines 0 and 3 is the reflex vertex. The vertex defined by the two lines not involved in defining the reflex vertex is the fixed vertex. Again, referring to Figure 10 the fixed vertex is defined by lines 5 and 9. The other four vertices are transient vertices. Of the transient vertices, the two vertices forming vertices of the convex hull are extruded vertices and the other two are intruded vertices. It is clear that the classification of a vertex is a constant time operation. Note that the classification of a vertex is only with respect to a specific facet; its classification may be different on a different facet.

Figure 10 also shows the resulting facet subgraph for each of the two interpretations. The quadrilateral  $afbe$  corresponds to the subgraph on the left, while the quadrilateral  $adbc$  corresponds to the subgraph on the right. Observe that the transient vertices are either both intruded or both extruded. Observe also that the internal angle at the reflex vertex is less than  $180^\circ$  (convex) if the intruded vertices are chosen and is greater than  $180^\circ$  (concave) if the extruded vertices are chosen.

Now we study the constraints provided by the adjacent facets. Observe that knowing any edge in the quadrilateral determines the complete quadrilateral since each edge has exactly one transient vertex incident to it. Consider a facet  $f_j$  adjacent to a facet  $f_i$ . If either the reflex vertex on facet  $f_i$  or the fixed vertex on facet  $f_i$  is a transient vertex on facet  $f_j$ , then facet  $f_j$  is completely determined. This in turn determines facet  $f_i$  and the other facets adjacent to facet  $f_i$  are completely determined. On the other hand, if the reflex vertex on facet  $f_i$  is the fixed vertex on facet  $f_j$ , facet  $f_i$  is completely determined and consequently all the facets adjacent to facet  $f_i$ .

Thus the only possibility for an ambiguous interpretation occurs when the fixed vertex on facet  $f_i$  is also the fixed vertex on an adjacent facet  $f_j$  and the reflex vertex on facet  $f_i$  is the reflex vertex on an adjacent facet  $f_k$ .

Suppose facet  $f_j$  is adjacent to facet  $f_i$  and they share the reflex vertex. If the convex internal angle at the reflex vertex in facet  $f_i$  is consistent with the convex internal angle at the reflex vertex in facet  $f_j$ , then again there is no ambiguity in determining the vertices

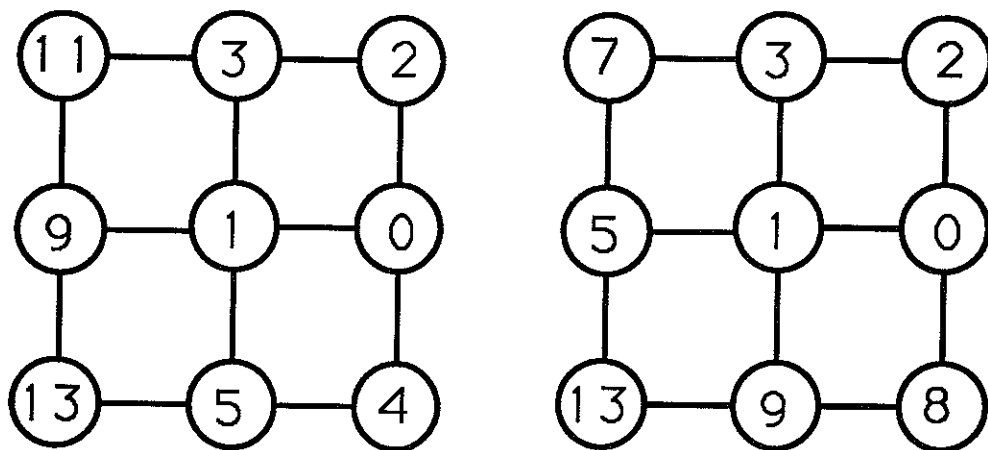
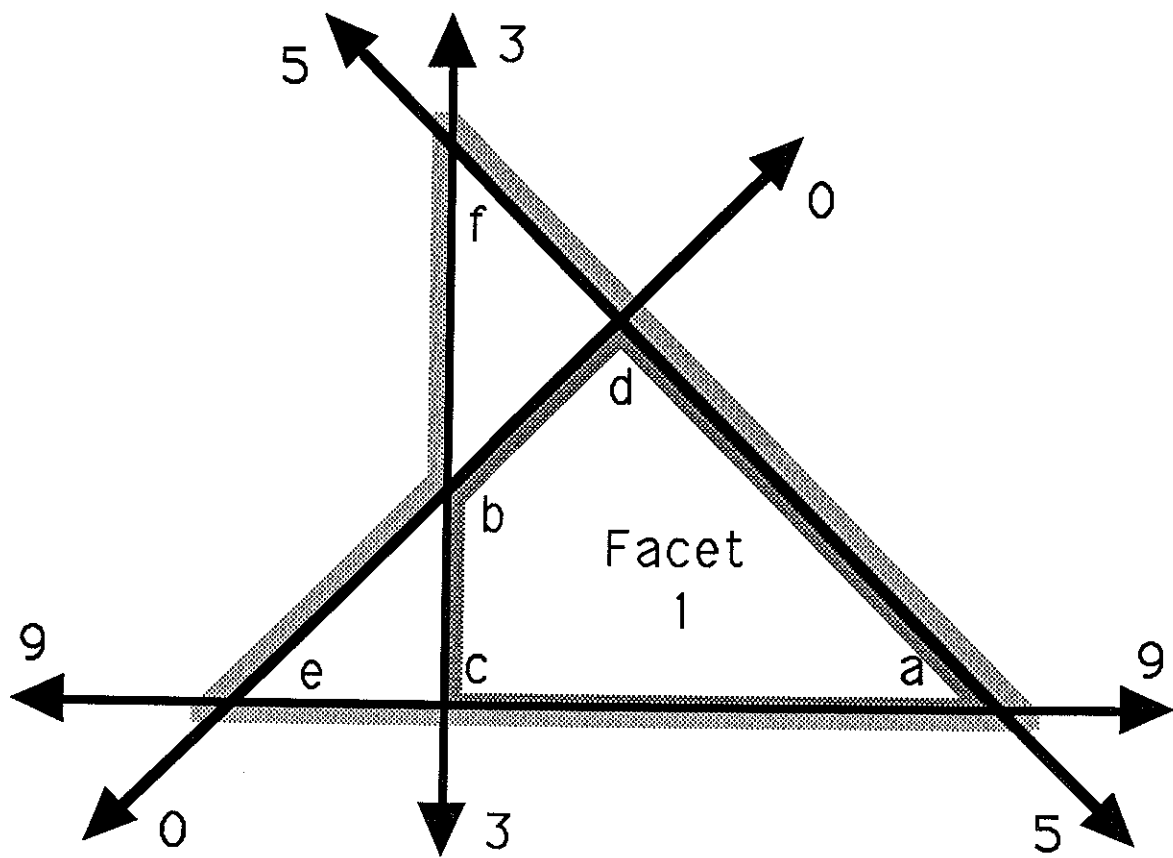


Figure 10: Two realizations of facet 1 and resulting subgraphs

and edges on facets  $f_i$  and  $f_j$ . This is evident when one observes that no two adjacent facets of a polyhedron can simultaneously have an internal angle greater than  $180^\circ$  at a common vertex.

Finally, ambiguity can continue to persist when the adjacent facets at a reflex vertex form an alternating sequence of convex and concave angles. Thus the transient vertices switch their classifications between adjacent facets, i.e., an intruded vertex on one facet is an extruded vertex on the adjacent facet.

The classification of the vertices in the four facets forming the reflex vertex is given in Figure 11. The fixed vertices are labeled  $p_i$ ,  $i = 1, \dots, 4$ , the reflex vertex is labeled  $O$ , and the transient vertices are labeled  $q_i$ ,  $i = 1, \dots, 8$ . As an example, the vertex defined by facets 1, 5, 0 and 4 is intruded on facet 1 and is extruded on facet 4.

Suppose a particular choice of the quadrilaterals on facet 1 is made. This completely determines the quadrilaterals of the four facets adjacent to it. Thus, once a particular choice at one facet has been made, the entire *SDR* of Figure 9 is determined.

**Lemma 6** *For every reflex vertex  $r$  of Figure 9, there is only one interpretation for each of its four facets.*

*Proof:* To obtain a contradiction, assume that there is a reflex vertex  $r$  with two interpretations. Without loss of generality, let the reflex vertex be  $r = (0, 0, 0)$  (labeled  $O$  for origin in Figure 11).

The following linear constraint equations can be obtained from Figure 11. (Note that these are 3-dimensional vector equations.)

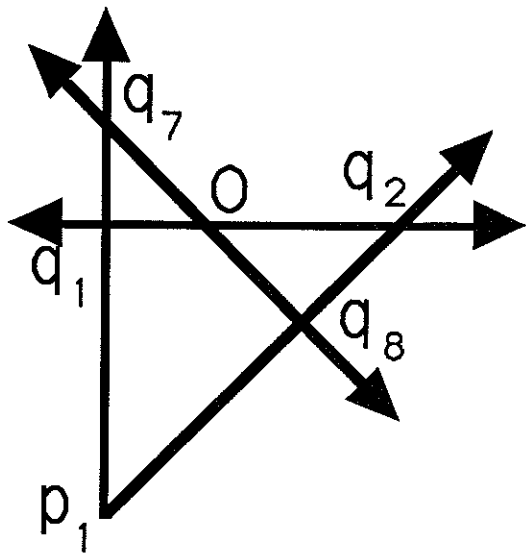
$$t_1(q_8 - p_1) = q_2 - p_1 \tag{2}$$

$$t_2(q_1 - p_1) = q_7 - p_1 \tag{3}$$

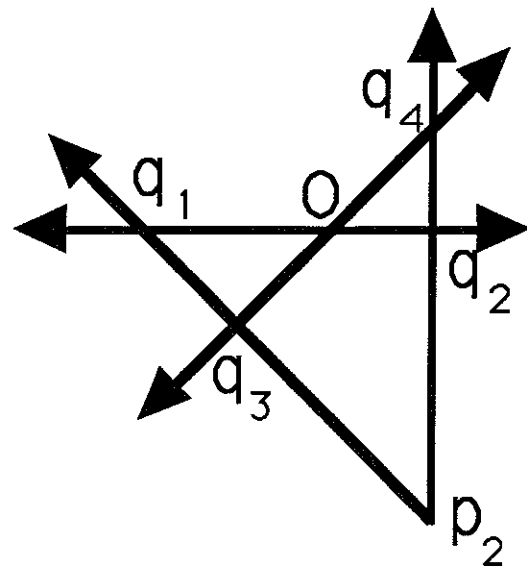
$$t_3(q_2 - p_2) = q_4 - p_2 \tag{4}$$

$$t_4(q_3 - p_2) = q_1 - p_2 \tag{5}$$

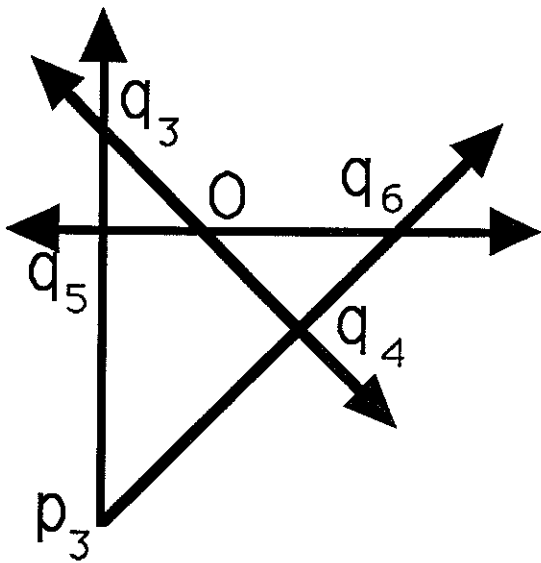




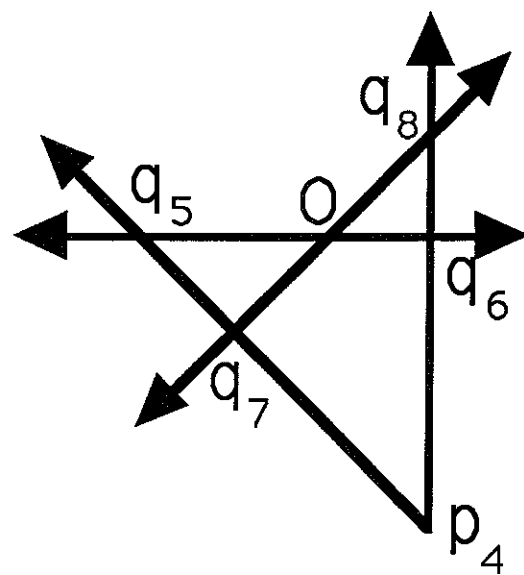
Facet 1



Facet 2



Facet 3



Facet 4

Figure 11: Four facets at a reflex vertex.

$$t_5(q_4 - p_3) = q_6 - p_3 \quad (6)$$

$$t_6(q_5 - p_3) = q_3 - p_3 \quad (7)$$

$$t_7(q_6 - p_4) = q_8 - p_4 \quad (8)$$

$$t_8(q_7 - p_4) = q_5 - p_4 \quad (9)$$

$$u_1 \cdot q_1 = q_2 \quad (10)$$

$$u_2 \cdot q_3 = q_4 \quad (11)$$

$$u_3 \cdot q_5 = q_6 \quad (12)$$

$$u_4 \cdot q_7 = q_8 \quad (13)$$

where for  $1 \leq i \leq 8$ ,  $t_i > 1$ , and for  $1 \leq i \leq 4$ ,  $u_i < 0$ . Eliminating  $p_1$  using Equations 2 and 3,  $p_2$  using Equations 4 and 5,  $p_3$  using Equations 6 and 7, and  $p_4$  using Equations 8 and 9, we obtain

$$\frac{(t_2 - 1)}{(t_1 - 1)}(t_1 q_8 - q_2) = t_2 q_1 - q_7 \quad (14)$$

$$\frac{(t_4 - 1)}{(t_3 - 1)}(t_3 q_2 - q_4) = t_4 q_3 - q_1 \quad (15)$$

$$\frac{(t_6 - 1)}{(t_5 - 1)}(t_5 q_4 - q_6) = t_6 q_5 - q_3 \quad (16)$$

$$\frac{(t_8 - 1)}{(t_7 - 1)}(t_7 q_6 - q_8) = t_8 q_7 - q_5 \quad (17)$$

Substituting for  $q_2, q_4, q_6$  and  $q_8$  from Equations 10, 11, 12 and 13 into Equations 14, 15, 16, and 17 and simplifying, we obtain

$$(t_2(t_1 - 1) + (t_2 - 1)u_1)q_1 - ((t_1 - 1) + (t_2 - 1)t_1 u_4)q_7 = 0$$

$$(t_4(t_3 - 1) + (t_4 - 1)u_2)q_3 - ((t_3 - 1) + (t_4 - 1)t_3 u_1)q_1 = 0$$

$$(t_6(t_5 - 1) + (t_6 - 1)u_3)q_5 - ((t_5 - 1) + (t_6 - 1)t_5 u_2)q_3 = 0$$

$$(t_8(t_7 - 1) + (t_8 - 1)u_4)q_7 - ((t_7 - 1) + (t_8 - 1)t_7 u_3)q_5 = 0.$$

Since no line passing through the pair of points appearing in any of the above 4 equations pass through the origin, the coefficient of each  $q_i$  in these equations is equal to zero. Thus we have

$$t_2(t_1 - 1) + (t_2 - 1)u_1 = 0 \quad (18)$$

$$(t_1 - 1) + (t_2 - 1)t_1 u_4 = 0 \quad (19)$$

$$t_4(t_3 - 1) + (t_4 - 1)u_2 = 0 \quad (20)$$

$$(t_3 - 1) + (t_4 - 1)t_3 u_1 = 0 \quad (21)$$

$$t_6(t_5 - 1) + (t_6 - 1)u_3 = 0 \quad (22)$$

$$(t_5 - 1) + (t_6 - 1)t_5 u_2 = 0 \quad (23)$$

$$t_8(t_7 - 1) + (t_8 - 1)u_4 = 0 \quad (24)$$

$$(t_7 - 1) + (t_8 - 1)t_7 u_3 = 0 \quad (25)$$

Substituting for  $u_1, u_2, u_3,$  and  $u_4$  from Equations 18, 20, 22, and 24 into Equations 21, 23, 25, and 19, respectively, gives

$$\begin{aligned} \frac{(t_3 - 1)}{(t_4 - 1)} &= t_2 t_3 \frac{(t_1 - 1)}{(t_2 - 1)} \\ \frac{(t_5 - 1)}{(t_6 - 1)} &= t_4 t_5 \frac{(t_3 - 1)}{(t_4 - 1)} \\ \frac{(t_7 - 1)}{(t_8 - 1)} &= t_6 t_7 \frac{(t_5 - 1)}{(t_6 - 1)} \\ \frac{(t_1 - 1)}{(t_2 - 1)} &= t_8 t_1 \frac{(t_7 - 1)}{(t_8 - 1)} \end{aligned}$$

which after further algebraic simplification yields

$$\frac{(t_1 - 1)}{(t_2 - 1)} = t_1 t_2 t_3 t_4 t_5 t_6 t_7 t_8 \frac{(t_1 - 1)}{(t_2 - 1)}$$

and finally

$$t_1 t_2 t_3 t_4 t_5 t_6 t_7 t_8 = 1.$$

This is a contradiction, since  $t_i > 1, i = 1, \dots, 8$ . The lemma follows.  $\square$

The arguments presented in this section can be generalized to the SDR of any polyhedron having degree  $\leq 4$ . As pointed out earlier, there cannot be any ambiguity in the interpretation of a quadrilateral formed by four arbitrary lines if any one of the transient vertices is known. Thus if any degree 4 facet  $f_i$  has a degree three facet adjacent to it,  $f_i$  is unambiguous. All degree 4 facets adjacent to  $f_i$  can then be resolved. Hence the SDR

of any polyhedron of maximum degree 4 with at least one node of degree 3 represents a unique polyhedron.

Now we show that there cannot be ambiguity at a reflex vertex which has an odd number of facets incident on it. Since there is a switch from convex to concave angles between the two interpretations, ambiguity at a reflex vertex with an odd number of facets would imply that there are at least two adjacent facets each of which has an internal angle greater than  $180^\circ$ . This is impossible in polyhedra. Thus there cannot be any ambiguity at a reflex vertex where an odd number of facets come together.

The remaining case to be considered is when an even number of facets come together at a reflex vertex, and all the nodes are of degree 4. We now prove that for this case also there is only one interpretation. The proof is a generalization of the proof of Lemma 6.

**Lemma 7** *An SDR of degree 4 with an even number of facets forming a reflex vertex represents a unique polyhedron.*

*Proof:* Let  $f_i$  be a facet involved in forming a reflex vertex and  $n$  the degree of the reflex vertex. Without loss of generality, we may assume that the reflex vertex is at the origin. The fixed vertex on  $f_i$  is  $p_i$ ,  $i = 1, \dots, n$ , while the intruded vertices are  $q_{2i-2}$  and  $q_{2i-1}$ . The extruded vertices are  $q_{2i}$  and  $q_{2i-3}$ . Subscripts are computed modulo  $2n$  with the caveat that 0 is represented by  $2n$ . The subscript arithmetic is unaffected by this variation. As an illustration, if there are 6 facets meeting at a reflex vertex, and we are considering the vertices on facet 1, then the intruded vertices are  $q_{12}$  and  $q_1$ , and the extruded vertices are  $q_2$  and  $q_{11}$  respectively. The line through the odd numbered vertices  $q_{2i-3}$  and  $q_{2i-1}$  passes through  $p_i$  and is formed by the intersection of  $f_i$  with one adjacent facet. Similarly, the line through the even numbered vertices  $q_{2i-2}$  and  $q_{2i}$  passes through  $p_i$ . See Figure 12. From the  $n$  facets meeting at the reflex vertex, the following relationships follow

$$t_{2i-1}(q_{2i-2} - p_i) = q_{2i} - p_i \quad (26)$$

$$t_{2i}(q_{2i-1} - p_i) = q_{2i-3} - p_i \quad (27)$$

$$u_i q_{2i-1} = q_{2i} \quad (28)$$

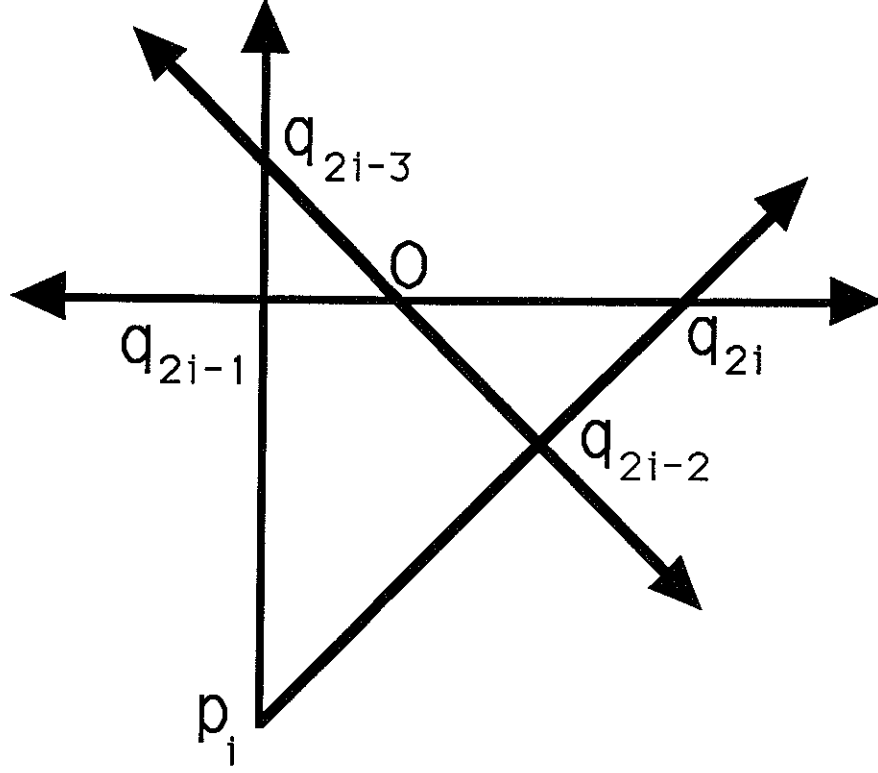


Figure 12: Vertex labeling of the realizations of facet  $f_i$ .

where  $t_{2i-1} > 1$ ,  $t_{2i} > 1$ ,  $u_i < 0$ ,  $i = 1, \dots, n$ . Substitute  $q_{2i}$  for  $i = 1, \dots, n$ , by  $u_i q_{2i-1}$  from Equation 28 into Equations 26 and 27 obtaining

$$\begin{aligned} & \left( t_{2i}(t_{2i-1} - 1) + (t_{2i} - 1)u_i \right) q_{2i-1} - \\ & \left( (t_{2i-1} - 1) + (t_{2i} - 1)t_{2i-1}u_{i-1} \right) q_{2i-3} = 0. \end{aligned} \quad (29)$$

From the geometry of the lines in Figure 12 and the fact that the origin is the reflex vertex, the coefficient of each point  $q_i$  in Equation 29 must be zero, i.e.,

$$t_{2i}(t_{2i-1} - 1) + (t_{2i} - 1)u_i = 0 \quad (30)$$

$$(t_{2i-1} - 1) + (t_{2i} - 1)t_{2i-1}u_{i-1} = 0. \quad (31)$$

Replace  $u_i$ ,  $i = 1, \dots, n$  in Equation 31 using Equation 30 obtaining

$$\frac{(t_{2i} - 1)}{(t_{2i-1} - 1)} = t_{2i} t_{2(i+1)-1} \frac{(t_{2(i+1)} - 1)}{(t_{2(i+1)-1} - 1)}$$

which yields

$$\frac{(t_2 - 1)}{(t_1 - 1)} = t_1 t_2 \dots t_{2n} \frac{(t_2 - 1)}{(t_1 - 1)},$$

and finally,

$$t_1 t_2 t_3 \dots t_{2n} = 1.$$

This is a contradiction, since  $t_i > 1$ ,  $i = 1, \dots, 2n$ . The lemma follows.  $\square$

Thus there cannot exist an even number of facets forming a reflex vertex such that every facet has two interpretations. Since there is no ambiguity at the reflex vertex, all the facets of the polyhedron are determined unambiguously and we have the following theorem.

**Theorem 8** *The SDR of a polyhedron of any genus is unambiguous if its degree is at most 4.*

*Proof:* Let facets  $f_i$  and  $f_j$  be adjacent in an SDR of maximum degree four. Facets  $f_i$  and  $f_j$  share an edge in the polyhedron represented by SDR. Let  $FV(f_k)$ ,  $RV(f_k)$ , and  $TV(f_k)$  be the fixed vertex, reflex vertex, and a transient vertex respectively on facet  $f_k$ . Assume that all the vertices on each facet have been classified as fixed, reflex or transient. We enumerate all possibilities, and show that for each possibility, the shapes of  $f_i$  and  $f_j$  are completely determined.

1. Either  $f_i$  or  $f_j$  is triangular: The triangular face is completely determined and consequently all its neighbors are determined.
2.  $FV(f_i) = TV(f_j)$ :  $f_j$  and consequently  $f_i$  and their neighbors are unambiguously determined.
3.  $RV(f_i) = TV(f_j)$ :  $f_j$  and consequently  $f_i$  and their neighbors are unambiguously determined.
4.  $RV(f_i) = FV(f_j)$ :  $f_i$  and then  $f_j$  and their neighbors are determined.

5.  $RV(f_i) = RV(f_j)$  and intruded  $TV(f_i) = \text{intruded } TV(f_j)$ :  $f_i$  and  $f_j$  are unambiguously determined, since one (impossible) choice requires both adjacent faces forming internal angles greater than  $180^\circ$  at the reflex vertex.
6.  $RV(f_i) = RV(f_j)$  and intruded  $TV(f_i) = \text{extruded } TV(f_j)$ :
  - An odd number of faces meet at the reflex vertex: Only one choice is possible since the alternate choice involves both the adjacent faces forming internal angles greater than  $180^\circ$ .
  - An even number of faces meet at the reflex vertex: By Lemma 7, there is only one choice.

□

The proof given above also provides an algorithm for reconstruction. Ambiguity at one reflex vertex is resolved using the above equations. This can be done in time proportional to the number of facets incident to the reflex vertex. The rest of the polyhedron is then reconstructed in time proportional to the size of the polyhedron. Thus the time complexity of the algorithm is  $O(n)$ , where  $n$  is the size of the *SDR*.

**Corollary 9** *The hypercube is unambiguous as an SDR.*

It is easy to observe that the hypercube can be interpreted as more than one polyhedron when viewed as a wire frame. The wire frame is a popular representation because of the perceptual ease of specifying a polyhedron in this representation scheme. The *SDR* is an equally easy representation to specify. One other advantage *SDR* enjoys over the wire frame representation is that the surface of a polyhedron is connected if and only if the *SDR* is connected. This is not the case for the wire frame representation. As a result we have the following theorem.

**Theorem 10** *SDR is a more powerful representation scheme than the wire frame when the degree of SDR is at most 4.*

## 6 Conclusion

Using the spherical dual representation, we have relaxed the requirement that the facet connectivity graph of a genus 0 polyhedron must be triconnected to support unique reconstruction. All genus 0 polyhedra are uniquely reconstructible. We have also extended unique reconstruction to any polyhedron of arbitrary genus, whose *SDR* has degree at most 4. The completeness of arbitrary spherical dual representations remains an open question. However, as numerous attempts to construct a polyhedron of higher genus that is a counterexample have failed, we are lead to the following conjecture:

**Conjecture 1** *The spherical dual representation of a polyhedron of arbitrary genus is uniquely reconstructible.*

This conjecture is the most intriguing question raised by this work. A resolution to this conjecture will require a deep understanding of the structure of planar-faced polyhedra of arbitrary genus. As a taste of what such understanding should entail, we offer this smaller conjecture:

**Conjecture 2** *No complete graph  $K_s$ ,  $s > 4$ , is the spherical dual representation of any planar-faced polyhedron.*

We also note that there is a *global* version of RECONSTRUCT that also reconstructs genus 0 polyhedra. It must consider what happens when an *SDR* is separated by a separation pair in the same manner as does RECONSTRUCT. We do not elaborate on this version as it is less likely to lead to a universal reconstruction algorithm for polyhedra of arbitrary genus.

We have already mentioned in the description of RECONSTRUCT how that algorithm can naturally extract many features (protrusions and depressions) of a solid. The lack of explicit order information in our approach is an advantage over the approach to feature extraction taken by Falcidieno and Giannini [3].



Another interesting aspect of our research has been the lack of the necessity for representing the adjacency information as a multigraph. In the light of our conjectures, we feel that the multigraph representation has the same power as the *SDR*.

An important observation is that RECONSTRUCT uses the requirement that facets are planar only to calculate  $\mathcal{Q}(f)$  and the edges of  $P$ . Therefore, RECONSTRUCT actually applies to larger classes of objects than we have allowed. It would be useful to specify and investigate other classes of “polyhedra” for which edges and the near-vertices in  $\mathcal{Q}(f)$  are easy to calculate.

## Acknowledgments

We wish to thank the two anonymous referees for a careful reading of the manuscript, which led to many improvements in the presentation.

## References

- [1] Edelsbrunner, H. *Algorithms in Combinatorial Geometry* (Springer-Verlag, Berlin, 1987).
- [2] Edmonds, J. A combinatorial representation for polyhedral surfaces, *American Mathematical Society Notices* (7) (1960) 646.
- [3] Falcidieno, B. and Giannini, F. Automatic recognition and representation of shape-based features in a geometric modeling system, *Computer Vision, Graphics, and Image Processing* (48) (1989) 93–123.
- [4] Gross, J. L. and Tucker, T. W. *Topological Graph Theory* (Wiley-Interscience Publication, New York, NY, 1987).
- [5] Grunbaum, B. *Convex Polytopes* (Interscience Publishers, London, 1967).

- [6] Hanrahan, P. Creating volume models from edge-vertex graphs, *Computer Graphics* (16) (1982) 77–84.
- [7] Hilbert, D. and Cohn-Vossen, S. *Geometry and the Imagination* (Chelsea Publishing, New York, NY, 1952).
- [8] Hopcroft, J. E. and Tarjan, R. E. Dividing a graph into triconnected components, *SIAM Journal on Computing* (2) (1973) 135–158.
- [9] Horn, B. K. P. *Robot Vision* McGraw-Hill Book Company, New York, NY, 1986
- [10] Huffman, D. A. Impossible objects as nonsense sentences, *Machine Intelligence, Volume 6* (American Elsevier Publishing Company, New York, NY, 1971) 295–324.
- [11] Huffman, D. A. A duality concept for the analysis of polyhedral scenes, *Machine Intelligence, Volume 8* (Ellis Horwood Limited, Chichester, England, 1977) 475–492.
- [12] Little, J. J. An iterative method for reconstructing convex polyhedra from extended gaussian image, *Proceedings of the National Conference on Artificial Intelligence* (1983) 247-250.
- [13] Mackworth, A. K. Interpreting pictures of polyhedral scenes, *Artificial Intelligence* (4) (1973) 121–137.
- [14] Mantyla, M. A note on the modeling space of Euler operators, *Computer Vision, Graphics and Image Processing* (26) (1984) 45–60.
- [15] Mantyla, M. *An Introduction to Solid Modeling* (Computer Science Press, Rockville, Maryland, 1988).
- [16] Markowsky, G. and Wesley, M.A. Fleshing out wire frames, *IBM Journal of Research and Development* (24) (1980) 582-597.
- [17] Paripati, P. *Polyhedra: Representation and Recognition*, M.S. thesis, Department of Computer Science, Virginia Polytechnic Institute and State University, Blacksburg, VA (1989).

- [18] Requicha, A. A. G. Representation of rigid solids—theory, methods and systems, *ACM Computing Surveys* (12) (1980) 437–464.
- [19] Roach, J. W., Wright, J., and Ramesh, V. Spherical dual images: a 3D representation method that combines dual space and Gaussian spheres, *IEEE 1986 Workshop on Computer Vision: Representation and Control* (1986) 236-241.
- [20] Roach, J. W., Paripati, P. and Wright, J. A CAD system based on spherical dual representations, *IEEE Computer* (20) (1987) 37–44.
- [21] Sabin, M. Geometric modelling: fundamentals, in: J. W. ten Hagen, ed., *Eurographics Tutorials '83* (Springer Verlag, Berlin, 1984) 343–389.
- [22] Shafer, S. A. *Shadows and Silhouettes in Computer Vision* (Kluwer Academic Publishers, Boston, 1985).
- [23] Tarjan, R. E. Depth first search and linear graph algorithms, *SIAM Journal on Computing* (1) (1972) 146–160.
- [24] Weiler, K. Edge based data structures for solid modeling in a curved surface environment, *IEEE Computer Graphics and Applications* (5) (1985) 21–40.
- [25] Whitney, H. Non-separable and planar graphs, *Transactions of the American Mathematical Society* (34) (1932) 339–363.